

Experimental study on preparation of calcium oxide by coal reduction of calcium sulfate in carbon dioxide atmosphere

Dong Ma  and Qinhui Wang ^{*}



Abstract

BACKGROUND: Recent studies show that CaO is being produced from CaSO₄ by CO reduction using fixed-bed reactors. However, the product yield is low and the reaction time is long. Furthermore, the high cost of CO hinders its application in industrial processes. Therefore, a new process is proposed for preparing CaO by CaSO₄ decomposition using lignite under CO₂. The influence of various process conditions on the production of CaO by CaSO₄ decomposition is investigated by combining kinetic and FactSage simulations. Finally, a typical industrial gypsum – phosphogypsum (PG) – is used for experimental verification.

RESULTS: The study found that adding CO₂ during the coal reduction of CaSO₄ increases the CaO yield. The ideal conditions are 1.75 C/Ca molar ratio, 7.5% CO₂ concentration at 1100 °C with the maximum CaSO₄ decomposition rate and CaO yield of 99.63% and 99.28%, respectively. CaO generation is carried out using a two-step process. Initially, CaSO₄ is reduced to become CaS and CaO, and CaS interacts with CaSO₄ to produce CaO. Secondly, the reaction between CaS and CO₂ produces CaO. The nucleation and growth model with $g(\alpha) = -\ln(1 - \alpha)$ is applicable to both processes. The experimental use of PG confirms the above conclusions, but SiO₂ in PG reacts with CaO to produce Ca₂SiO₄ and affect the CaO yield.

CONCLUSION: The addition of CO₂ promotes the conversion process of CaSO₄ to CaO. Increasing the temperature, C/Ca molar ratio and CO₂ concentration favor the decomposition of CaSO₄ into CaO. This study offers advice for using CaSO₄ products like PG as resources.

© 2023 Society of Chemical Industry (SCI).

Supporting information may be found in the online version of this article.

Keywords: calcium sulfate; carbon dioxide; lignite; calcium oxide; phosphogypsum; kinetics

INTRODUCTION

Due to the development of various industries such as construction, agriculture and chemical manufacturing, China's industrial gypsum production has increased in recent years. According to statistics, China's annual industrial gypsum production is about 155 million tons, including 55 million tons of phosphogypsum (PG) and 100 million tons of desulfurization gypsum.¹ The main component of PG and desulfurization gypsum is CaSO₄.nH₂O ($n = 0.5, 1, 1.5, 2$).² However, compared with desulfurization gypsum, PG is more difficult to handle. Due to its radioactive elements, long-term accumulation or improper treatment of PG can cause serious environmental pollution, so the treatment and comprehensive utilization of PG is a very important task.³ Currently, the utilization of PG is mainly focused on traditional building materials, cement and other fields, but its comprehensive utilization rate needs to be improved. To minimize its negative effects on the environment and increase the value of its resources, it is vital to create efficient usage methods.

As a significant chemical raw material, lime is an essential component in the creation of goods such as glass, gypsum and cement. In agriculture, lime is also used as a soil conditioner to neutralize soil acidity and improve soil structure. Lime is used to clean exhaust gas and wastewater in the realm of environmental

protection.⁴ CaO is the primary ingredient of lime. In traditional industries, lime is primarily produced by calcining limestone at temperatures of 800–1100 °C. The calcination of limestone produces a large amount of CO₂. According to statistics, the amount of CO₂ emitted annually from the calcination of limestone in China is approximately 10% of the global total CO₂ emissions, making it the third-largest source of CO₂ emissions in China. Among them, CO₂ emissions from the calcination of industrial limestone account for about 70% of the total emissions.⁵ As a result, creating low-CO₂-emission manufacturing techniques for lime has emerged as a significant problem in the realm of environmental protection in order to meet carbon neutrality objectives.

Converting CaSO₄ from PG into CaO through thermochemical methods not only achieves efficient utilization and recycling of waste resources, avoiding long-term accumulation and potential environmental hazards, but also fully utilizes useful elements such

* Correspondence to: Qinhui Wang, State Key Laboratory of Clean Energy Utilization, Institute for Thermal Power Engineering, Zhejiang University, Hangzhou 310027, China. E-mail: qinhui_wang@126.com

State Key Laboratory of Clean Energy Utilization, Institute for Thermal Power Engineering, Zhejiang University, Hangzhou, China

as calcium and sulfur. In addition, compared with traditional limestone calcination, CO₂ emissions are significantly reduced. While CaSO₄ decomposes at temperatures of up to 1400 °C, introducing reducing agents can drastically lower this temperature.⁶ Common reducing agents mainly include carbon-based (lignite,⁷ anthracite,⁸ coke,⁹ coal gangue,¹⁰ CO¹¹) and sulfur-based (sulfur,¹² pyrite,¹³ H₂S¹⁴). Therefore, the conversion of CaSO₄ to CaO is completely feasible in terms of process. Many studies are being done on the production of CaO from the decomposition of CaSO₄. Xia *et al.*¹⁵ discovered that when reaction time was 2 h temperature was above 1000 °C, CO volume concentration exceeded 2% and CO₂/CO partial pressure ratio exceeded 8 in a vertical fixed bed, CaO might be produced entirely from CaSO₄. The presence of O₂ was beneficial to the improvement of CaO yield, and the CaO prepared by this method was superior to the CaCO₃ method. According to research done by Okumura *et al.*¹⁶ on the CaSO₄ decomposition in a packed-bed reactor, the CO/CO₂ concentration ratio had a significant impact on CaSO₄ decomposed to CaO. At 1000 °C and in a gas atmosphere of 2% CO and 30% CO₂, the CaO yield was 91%. Using thermogravimetric isothermal experiments, Xiao *et al.*¹⁷ investigated the decomposition process of CaSO₄ under various CO volume fractions and discovered that it was a parallel competitive reaction. As the CO concentration increased, CaO was gradually converted to CaS. Density functional theory was used by Zhang *et al.*¹⁸ to investigate the process by which CaSO₄ was reduced and broken down by CO. It was discovered that at lower reaction temperatures and higher CO and CaSO₄ molar ratios CaS was the main product. When the temperature rose and the molar ratios of CO and CaSO₄ declined, CaO was the main product. In their investigation of the reduction of PG with high sulfur coal in a fixed bed, Zheng *et al.*¹⁹ discovered that the CaO concentration was 57.13% and its highest SO₂ concentration was 7.6%, with a C/Ca molar ratio of 1.2 at 1000 °C. According to research by Xu *et al.*,²⁰ the maximum rates of PG decomposition and desulfurization were 97.73% and 97.2%, respectively, at 1180 °C for 15 min with 4% carbon content and 6% CO concentration. Zhang *et al.*²¹ used a thermogravimetric analyzer to study the process of coal reduction of PG in a CO₂ atmosphere. It was found that when Ca/C = 0.5, the main solid product was CaS and less SO₂ was released. When Ca/C = 2, the CaO content increased and the SO₂ concentration in the gas increased.

In summary, thermogravimetric analysis or fixed-bed reactors are primarily used in current research on the production of CaO by reducing CaSO₄ with CO. However, the process frequently takes a long time and has a low yield of product because fixed-bed reactor heat and mass transport are inefficient. In addition, the high cost of CO also hinders its practical application in industrial processes. Therefore, this study proposes the use of lignite as a reducing agent under CO₂ atmosphere. By combining FactSage thermodynamic simulation and kinetic calculation, the influence of reaction temperature, C/Ca molar ratio and CO₂ concentration on the CaSO₄ decomposition process to prepare CaO is investigated to obtain optimized reaction conditions. Finally, typical industrial waste products, PG and desilication PG, are used to

study their reaction characteristics under CO₂ and coal conditions. This study provides practical guidance for the resource utilization of CaSO₄ waste products such as PG.

EXPERIMENTAL

Experimental raw materials

Anhydrous CaSO₄ of analytical grade purity and fewer than 0.075 mm-sized particles was acquired from Macklin Company. PG was provided by a phosphorus chemical company in Yunnan, China. Because of the high water content of the PG sample, it was dried at 80 °C to a constant weight to remove free water, crushed and sieved; particles smaller than 0.075 mm were selected and stored in a sealed container. The above PG was subjected to silicon removal treatment by a chemical method and then stored in a sealed container. The findings of the chemical composition of PG and desilicated PG using X-ray fluorescence spectrometry (XRF; Shimadzu, Kyoto, Japan) are displayed in Table 1.

The analysis results show that PG contained mainly CaO and SO₃, 1.36% SiO₂, as well as small amounts of Al₂O₃, P₂O₅, F and organic matter. The silicon content in desilicated PG was significantly reduced. Phase analysis of PG was performed using X-ray diffraction (XRD; Ultima IV, Rigaku, Tokyo, Japan). The spectra are displayed in Supporting Information, Fig. S1. It has been discovered that SiO₂, CaSO₄·2H₂O and CaSO₄·0.5H₂O are the major components of PG.

The coal used in the experiment was Yunnan Anning lignite, which was first dried at 80 °C to constant weight. The lignite was crushed and sieved to choose particles with a size of 0.075–0.15 mm for storage in order to simplify coal and product separation. The dried coal was subjected to industrial analysis and elemental analysis tests based on GB/T 212-2008 and GB/T 31391-2015. The results are shown in Table 2.

Product composition determination

Solid samples were collected and stored following the experiments. The barium sulfate precipitation technique (GB/T 5484-2012) was used to determine CaSO₄ content. The methylene blue spectrophotometric technique (HJ 1226-2021) was used to determine CaS concentration. The sucrose technique (HG/T 4205-2011) was used to determine CaO concentration. Product composition was determined by XRD. Equations (1)–(3) show the specific computation technique:

$$\varphi_{\text{CaSO}_4} = \frac{m_o \times X_{\text{O,CaSO}_4} - m_t \times X_{\text{t,CaSO}_4}}{m_o \times X_{\text{O,CaSO}_4}} \times 100\% \quad (1)$$

$$\phi_{\text{CaS}} = \frac{m_t \times X_{\text{t,CaS}}}{Q_{\text{CaS}}} \times 100\% \quad (2)$$

$$\phi_{\text{CaO}} = \frac{m_t \times X_{\text{t,CaO}}}{Q_{\text{CaO}}} \times 100\%. \quad (3)$$

The symbols in the equations are defined as follows: φ_{CaSO_4} denotes the CaSO₄ decomposition rate, %, m_o and m_t denote

Table 1. Chemical composition of phosphogypsum (PG) and desilicated PG (%)

Sample	SiO ₂	SO ₃	CaO	Fe ₂ O ₃	Al ₂ O ₃	MgO	Na ₂ O	K ₂ O	P ₂ O ₅	Total F	Organic matter
PG	17.25	47.87	33.51	0.54	0.51	0.25	0.16	0.23	0.61	0.22	0.31
Desilicated PG	1.36	56.40	39.48	-	0.15	0.09	0.20	0.21	0.38	0.13	0.24

Table 2. Main characteristics of samples

Sample	Industrial analysis, wt%				Elemental analysis, wt%				
	M_{ad}	A_d	V_d	FC_d	C_{ad}	H_{ad}	O_{ad}^*	N_{ad}	$S_{t,ad}$
Coal	5.07	18.84	46.62	34.54	54.10	4.45	20.72	1.33	0.56

*By difference.

the raw material and product masses, respectively, g, $X_{o,CaSO_4}$ and $X_{t,CaSO_4}$ denote the proportion of $CaSO_4$ in the raw material and product, respectively, %, $X_{t,CaS}$ and $X_{t,CaO}$ denote the CaS and CaO proportions in the product, respectively, %, Q_{CaS} denotes the theoretical mass of CaS produced from the complete conversion of $CaSO_4$, g, Q_{CaO} denotes the theoretical mass of CaO produced from the complete conversion of $CaSO_4$, g.

Small fluidized bed experiment

Figure 1 depicts the small-scale fluidized bed reactor used for the experiment. A quartz tube with a length of 1 m and a diameter of 50 mm is arranged in the fluidized bed. A 0.45 μm aperture air distribution plate is set in the middle of the quartz tube. A valve system is built on top of the feeding funnel to create a storage chamber for reaction particles, preventing materials from being transported out of the reactor. The electric furnace's temperature control system is employed to accurately regulate the reaction's temperature. The CO_2 and N_2 used in the experiment are both 99.999% high-purity gases. The mass flow meter (CS200, Beijing Qixing, China) is used to accurately control the flow rate of the reaction gas. The total gas flow rate is controlled at 2 L/min during the experiment. Cold-state experiments show that the material in the reactor could achieve uniform fluidization when the fluidization air flow rate is 2 L/min. The concentration of SO_2 is measured using a portable infrared flue gas analyzer (MGA6plus, MRU, Germany), with sampling and analysis conducted every 5 s.

Thermodynamic simulation

Based on the idea of lowest Gibbs free energy, the FactSage 6.0 software calculates thermodynamic equilibrium. The thermodynamic

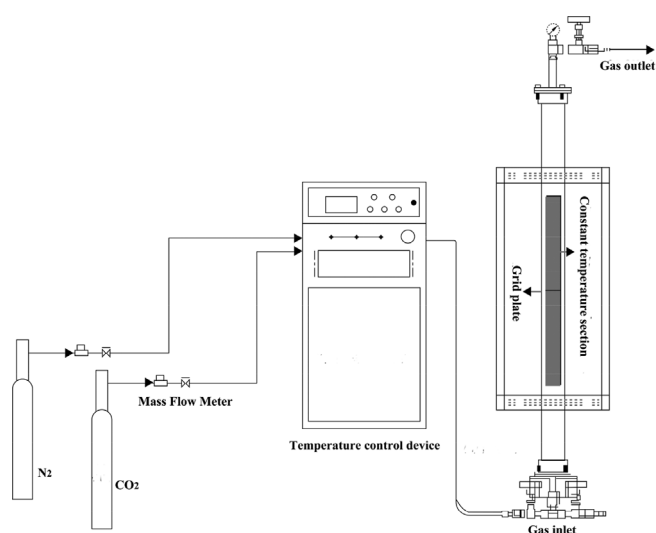


Figure 1. Fluidized bed reactor schematic diagram.

process is primarily examined in this paper using the Phase Diagram Module. The reactant types are set to solid and gas at the starting pressure of 0.1 MPa. The product composition is investigated under different $C/(C + Ca)$ molar ratios, and CO_2 partial pressures.

Thermogravimetric experiment

The thermogravimetric analyzer used in the experiment is Netzsch STA 409PC from Germany (sensitivity of 2 μg and temperature accuracy of $<1^\circ C$). $CaSO_4$ and coal powder are thoroughly ground and used for the subsequent experiment with a C/Ca molar ratio of 1.75. A sample weighing 10 mg is taken and the experiment is conducted in a mixture of CO_2/N_2 . The sweeping gas is N_2 at a flow rate of 50 mL/min, while the CO_2 flow rate is 20 mL/min. The ultimate experiment temperature is 1250 $^\circ C$, and the program's heating speeds are 10, 15, and 20 $^\circ C/min$. The kinetic parameters at different heating rates are calculated using the Flynn-Wall-Ozawa (FWO) and Kissinger-Akahira-Sunose (KAS) methods, as described in the supporting information.

RESULTS AND DISCUSSION

FactSage simulation results

Using the module of phase diagram in FactSage thermodynamic software, the equilibrium phase diagrams of products during coal reduction of $CaSO_4$ are investigated, as shown in Fig. 2. Figure 2(a) displays the influence of the reactant molar ratio $C/(C + CaSO_4)$ on the decomposition products of $CaSO_4$ within 800–1800 $^\circ C$. The findings show that temperature and carbon content significantly affect the product composition. The minimum temperature for pure CaO phase appearance in the coal reduction of $CaSO_4$ process is about 1120 $^\circ C$, when the $C/(C + CaSO_4)$ molar ratio is approximately 0.35. The region of pure CaO phase steadily rises as temperature and carbon concentration rise. In the temperature range of 800–1800 $^\circ C$, Fig. 2(b) examines the impact of adding CO_2 to the reaction atmosphere on the $CaSO_4$ decomposition products. The area of pure CaO in the equilibrium phase diagram is significantly expanded by the addition of CO_2 in comparison to the absence of CO_2 . Consequently, the manufacture of CaO by coal reduction of $CaSO_4$ is facilitated by the addition of CO_2 . Figure 2(c,d) further explore the distribution of products in $CaSO_4-C-N_2$ and $CaSO_4-C-CO_2$ systems at 1100 $^\circ C$. The findings demonstrate that the region of pure CaO phase rises with the addition of CO_2 . This conclusion will provide theoretical guidance for subsequent experimental verification.

Influence of temperature

Based on thermodynamic analysis, the impact of temperature (950 ~ 1100 $^\circ C$) on the rate of $CaSO_4$ decomposition and CaO yield in the $CaSO_4-C$ and $CaSO_4-C-CO_2$ systems is investigated. The C/Ca molar ratio, CO_2 concentration, and reaction duration are all kept at 1.75, 7.5%, and 1 h, respectively. The findings are displayed in Fig. 3.

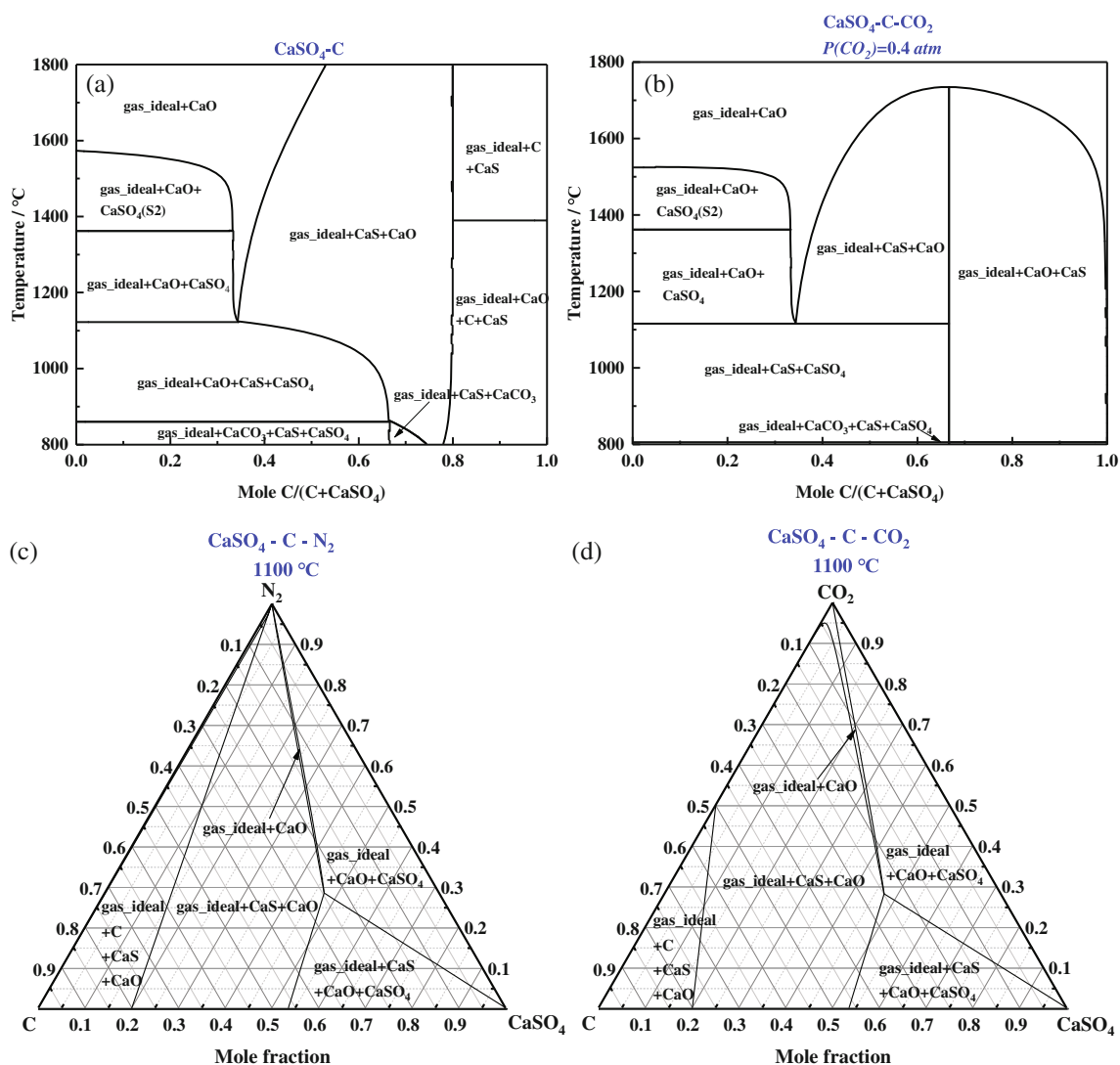


Figure 2. (a) Binary equilibrium phase diagram of $\text{CaSO}_4\text{--C}$, (b) Binary equilibrium phase diagram of $\text{CaSO}_4\text{--C--CO}_2$, (c) Ternary equilibrium phase diagram of $\text{CaSO}_4\text{--C--N}_2$, (d) Ternary equilibrium phase diagram of $\text{CaSO}_4\text{--C--CO}_2$.

The rate at which CaSO_4 decomposes in both the $\text{CaSO}_4\text{--C}$ and $\text{CaSO}_4\text{--C--CO}_2$ systems is greatly increased by raising the reaction temperature, as shown in Fig. 3(a). For instance, in the $\text{CaSO}_4\text{--C--CO}_2$ system, when the temperature climbs from 950 °C to 1100 °C, the rate of CaSO_4 decomposition jumps from 75.56% to 99.63%. The CaSO_4 decomposition rate rises for the $\text{CaSO}_4\text{--C}$ system from 65.27% to 99.67%. At a temperature of 1100 °C, CaSO_4 in both systems is completely decomposed. Moreover, at the same temperature, the $\text{CaSO}_4\text{--C--CO}_2$ system exhibits a greater rate of CaSO_4 decomposition than the $\text{CaSO}_4\text{--C}$ system. This might be as a result of the fact that 1 mol coal combines with CO_2 to produce 2 mol carbon monoxide, which then takes part in the reaction with CaSO_4 to make CaO , as stated in Eqn (4) and (5).

The yield of CaO in two systems at various temperatures is compared in Fig. 3(b). It is obvious that raising the temperature considerably increases the CaO production. For instance, the CaO yield in the $\text{CaSO}_4\text{--C--CO}_2$ system increases from 62.34% to 99.28% when the temperature is raised from 950 °C to 1100 °C. This indicates that at 1100 °C, CaSO_4 has completely decomposed into CaO . The CaO yield for the $\text{CaSO}_4\text{--C}$ system rises from 32.23%

to 64.78%. Moreover, at the same temperature, the CaO yield in the $\text{CaSO}_4\text{--C}$ system is much lower than it is in the $\text{CaSO}_4\text{--C--CO}_2$ system. This suggests that the yield of CaO can be increased by adding CO_2 .

Figure 3(c) displays the XRD spectra of the two systems' products at various temperatures. It is evident that CaSO_4 in both systems mostly decomposes into CaS and CaO at 950 °C. With increasing temperature, the characteristic peaks of CaSO_4 and CaS in both systems decrease, while the characteristic peak of CaO increases. At 1100 °C, the CaSO_4 in the $\text{CaSO}_4\text{--C--CO}_2$ system has completely transformed into CaO , while the product of the $\text{CaSO}_4\text{--C}$ system still contains a significant amount of CaS . This result explains the experimental conclusions in Fig. 3(a) and Fig. 3(b).

Figure 3(d) depicts how the SO_2 concentration changes over time in the $\text{CaSO}_4\text{--C--CO}_2$ system at various temperatures. The process of SO_2 emission is significantly influenced by temperature, as can be shown. The emission of SO_2 proceeds more quickly and SO_2 peak concentration rises noticeably with rising temperature. This suggests that raising the temperature makes CaSO_4 breakdown more feasible. In addition, at 1050 and 1100 °C, two

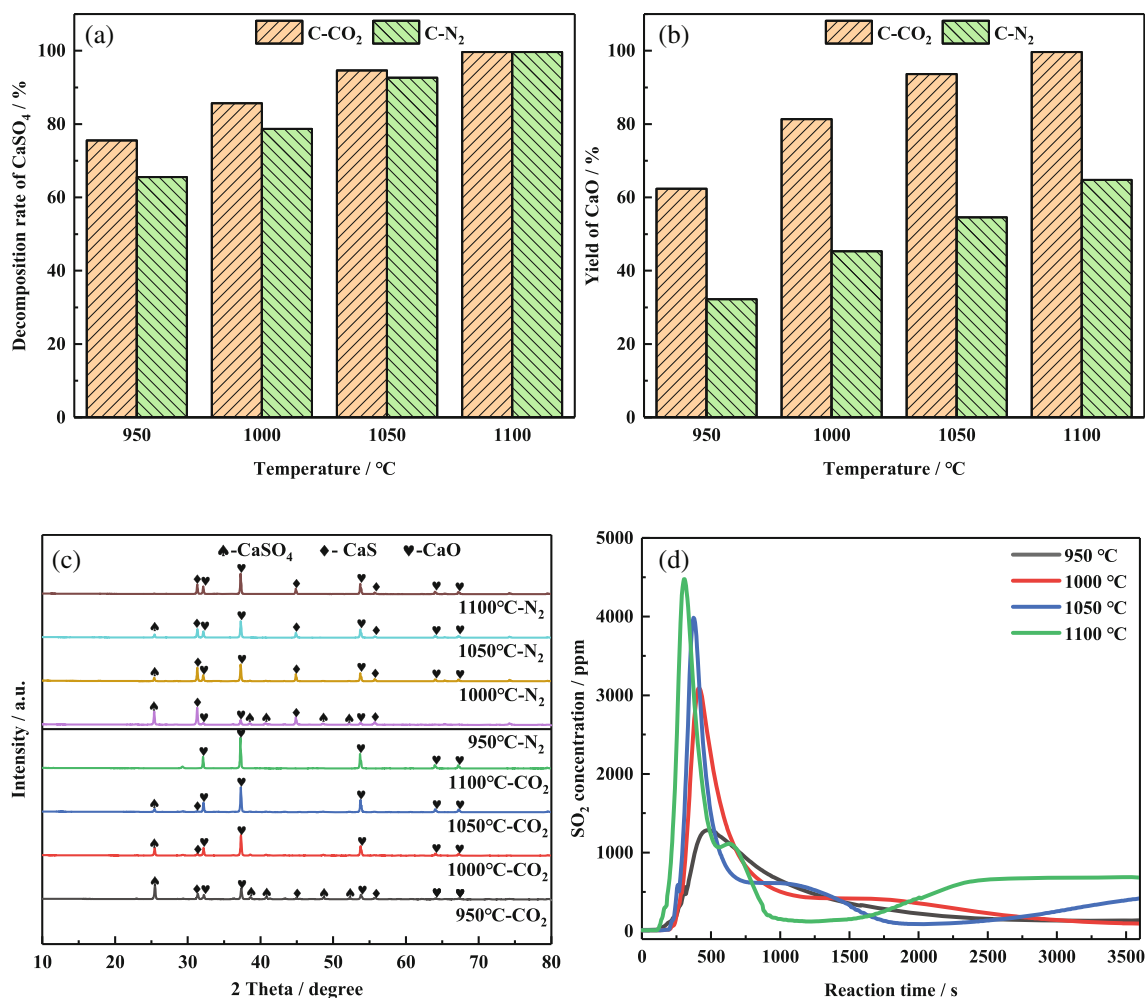
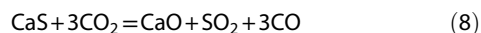
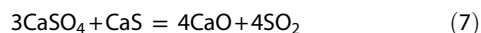
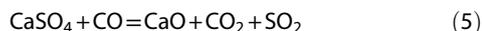


Figure 3. (a) Influence of temperature on the rate of CaSO₄ decomposition, (b) Influence of temperature on the CaO yield, (c) X-ray diffraction patterns of products at different temperatures, (d) Variation curves of SO₂ concentration with reaction time at different temperatures.

obvious concentration increase processes of SO₂ can be observed, while only one obvious concentration increase process can be observed at 950 and 1000 °C. The first increase in SO₂ concentration is caused by reactions (5)–(7),²² and the second increase in concentration is caused by reaction 8.²³ This is because the spontaneous reaction temperatures of reaction 5 and reaction 6 are 811 and 924 °C, respectively, and reaction 7 can occur through the liquid phase co-melting model at 950 °C,²⁴ while reaction 8 can only occur spontaneously at temperatures above 1000 °C.



Influence of the C/Ca molar ratio

The influence of the C/Ca molar ratio is next examined with regard to the production of CaO and the rate at which CaSO₄ decomposes in the CaSO₄–C and CaSO₄–C–CO₂ systems. With the

temperature of 1100 °C and CO₂ concentration of 7.5%, the experimental reaction time is regulated to 1 h. Figure 4 exhibits the findings.

The decomposition of CaSO₄ is aided by adding more coal, as seen in Fig. 4(a). For the CaSO₄–C–CO₂ system, the CaSO₄ decomposition rate rises from 42.96% to 99.63% when the C/Ca molar ratio increases from 0.25 to 0.75. The CaSO₄ decomposition rate increases from 38.46% to 99.67% in the CaSO₄–C system. The CaSO₄–C–CO₂ system decomposes CaSO₄ at a rate that is noticeably greater than the CaSO₄–C system at the same C/Ca molar ratio. Reaction (4) and (5) can explain the reason for this. Under the same carbon content, carbon and carbon dioxide can produce more CO gas, which is more conducive to the reduction process of CaSO₄.

As shown in Fig. 4(b), increasing the coal content has different effects on CaO yield in the two systems. The CaO yield in the CaSO₄–C–CO₂ system increases from 42.37% to 99.28% when the C/Ca molar ratio increases from 0.25 to 0.75. When compared to the CaSO₄ decomposition rate, it can be seen that the CaO yield and CaSO₄ decomposition rate are nearly identical, proving that the decomposed CaSO₄ has been nearly entirely converted into CaO. While the C/Ca molar ratio in the CaSO₄–C system increases, the CaO yield shows an initial increase and then a decrease. The reason may be that when the C/Ca molar ratio is relatively low,

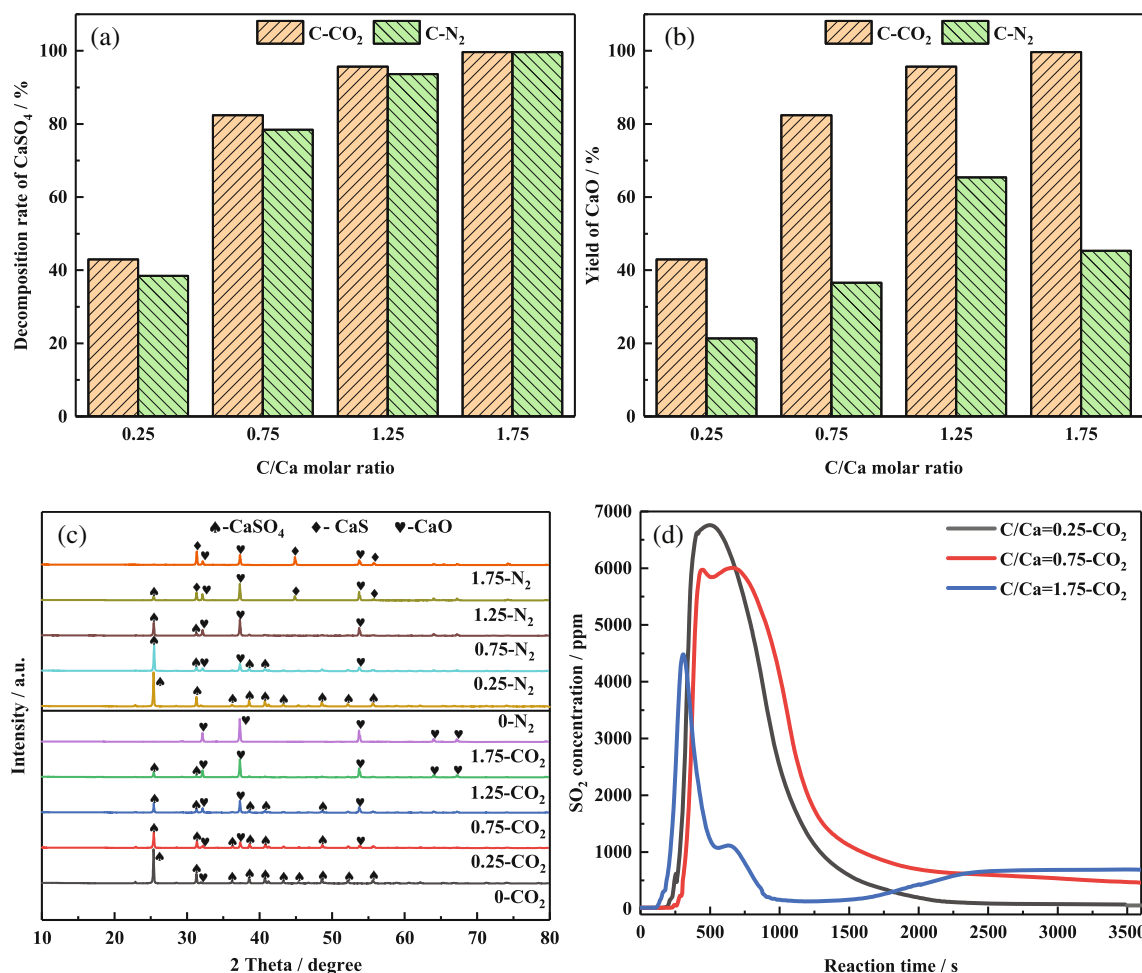


Figure 4. (a) Influence of C/Ca molar ratio on the rate of CaSO₄ decomposition, (b) Influence of C/Ca molar ratio on the CaO yield, (c) Influence of C/Ca molar ratio on product components, (d) Variation curve of SO₂ concentration with reaction time at C/Ca molar ratio.

CaSO₄ cannot be completely decomposed into CaS and CaO, leading to the further reaction of CaS with CaSO₄ to generate CaO at 1100 °C, resulting in an increase in CaO yield. Studies have shown that there is a competitive reaction between CaS and CaO, the decomposition products of CaSO₄.²⁵ CaS is the primary decomposition product of CaSO₄ at high C/Ca molar ratios. As a result, CaSO₄ is mostly converted to CaS when the C/Ca molar ratio rises, which lowers the CaO yield.

The XRD spectra of the products in Fig. 4(c) also support the conclusions drawn above. When the C/Ca molar ratio grows for the CaSO₄-C system from 0.25 to 1.25, the distinctive peak intensity of CaSO₄ dramatically declines while CaO significantly increases, suggesting that CaSO₄ is continually degraded and changed into CaO. As the C/Ca molar ratio is raised further to 1.75, a distinct CaS characteristic peak appears in the product, and the CaO peak intensity decreases significantly, indicating that CaSO₄ gradually transforms into CaS and results in a decrease in CaO yield. For the CaSO₄-C-CO₂ system, as the C/Ca molar ratio increases, the CaSO₄ peak intensity continuously decreases, while the CaO characteristic peak intensity increases continuously, and no obvious CaS characteristic peak is observed in the product, indicating that CaS is oxidized to SO₂ by CO₂, producing CaO and resulting in an increase in CaO yield.

Figure 4(d) shows the variation of SO₂ concentration over time in the CaSO₄-C-CO₂ system at different C/Ca molar ratios. It can be observed that there are two distinct periods of SO₂

concentration increase at the C/Ca molar ratio of 1.75. However, when the C/Ca molar ratio is lower, only one period of SO₂ concentration increase is observed. The reason is that at lower coal content, the main decomposition products of CaSO₄ are CaO and SO₂. At higher coal content, the main decomposition products of CaSO₄ are CaS and a small amount of CaO. Subsequently, CaS continues to react with CO₂ to produce SO₂ and CaO. Therefore, at a higher C/Ca molar ratio, two distinct periods of SO₂ concentration increase are observed.

Influence of CO₂ concentration

Next, it is determined how CO₂ concentration (0–10%) affects the rate of CaSO₄ decomposition and CaO yield in the CaSO₄-C system. The reaction temperature is maintained at 1100 °C, the C/Ca molar ratio is 1.75, and the reaction time is controlled at 1 h. The findings are displayed in Fig. 5.

Figure 5(a) shows that the decomposition rate of CaSO₄ has reached 99.23% in the absence of CO₂ and that the rate of decomposition is not significantly affected by an increase in CO₂ concentration. However, CaO production did increase significantly with increasing CO₂ concentration. The CaO yield increases from 64.78% to 99.28% when the CO₂ concentration goes from 0% to 7.5%, and further raising the CO₂ concentration has no effect on the CaO yield.

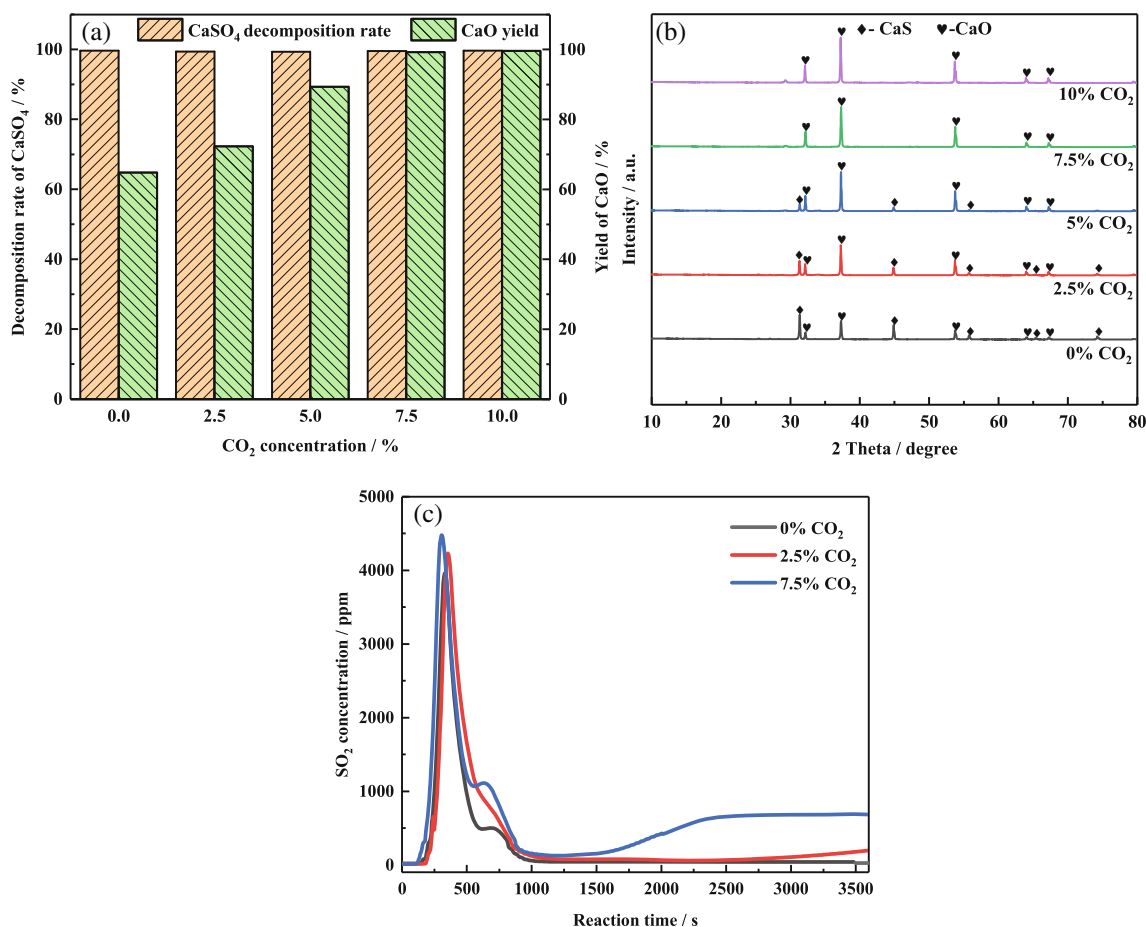


Figure 5. (a) Influence of CO₂ concentration on the rate of CaSO₄ decomposition and the production of CaO, (b) X-ray diffraction patterns of products at different CO₂ concentrations, (c) Variation curves of SO₂ concentration with reaction time at different CO₂ concentrations.

The XRD patterns of the products exhibited in Fig. 5(b) further support this conclusion. The primary breakdown products of CaSO₄ without the addition of carbon dioxide are CaS and CaO. With increasing CO₂ concentration, CaS is gradually transformed into CaO. When the CO₂ concentration reaches 7.5%, all decomposition products of CaSO₄ are CaO.

Figure 5(c) depicts the CaSO₄-C system's SO₂ concentration variation over time at various CO₂ concentrations. It can be observed that without the addition of CO₂, the SO₂ curve exhibits only one clear concentration increase stage. As the CO₂ concentration increases to 2.5%, a second concentration increase stage appears in the SO₂ curve. With further increase in CO₂ concentration to 7.5%, the second concentration growth process becomes rapid. This shows that CaS is oxidized by CO₂ to CaO, which increases the amount of SO₂.

Reaction mechanism

As a result, a mechanistic analysis of the CaSO₄ reduction by coal to prepare CaO in a CO₂ atmosphere is carried out. Measurements of the product composition are made every 10 min during the experiments, which are carried out at a reaction temperature of 1100 °C, a C/Ca molar ratio of 1.75, and a CO₂ concentration of 7.5%. The findings are displayed in Fig. 6.

From Fig. 6(a), CaSO₄ continuously decomposes into CaS and CaO during the reaction. After 10 min, the proportions of CaSO₄,

CaS, and CaO in the product are 43.13%, 34.53%, and 22.34%, respectively. After 20 min, the proportions are 10.68%, 46.90%, and 42.42%, respectively. When the reaction reaches 30 min, the proportion of CaSO₄ has decreased to 0.38%, and the proportion of CaO has increased to 62.42%, while the proportion of CaS has decreased to 37.20%. The proportion of CaS gradually decreases and the proportion of CaO gradually increases as the reaction time is extended. The XRD pattern seen in Fig. 6(b) adds the support for this finding. As response time grows, the intensity of the typical CaSO₄ peak progressively declines, the intensity of the characteristic CaS peak fluctuates before decreasing, and the intensity of the characteristic CaO peak steadily climbs. Consequently, it may be concluded that CaS is a byproduct of the intermediate stage of CaSO₄ decomposition. As the reaction develops, CaS keeps reacting with unreacted CaSO₄ to produce CaO and SO₂. After CaSO₄ is completely decomposed, CaS continues to react with CO₂ to generate CaO. This result is consistent with the trend of the concentration curve of SO₂ with time mentioned earlier.

Dynamical analysis

Figure 7 displays the thermalgravimetric (TG)- derivative thermalgravimetric (DTG) curves for the CaSO₄-C-CO₂ system at various heating rates. Figure 7(a) demonstrates how the TG curve shifts towards higher temperatures as the heating rate rises. The effect of 'thermal delay' is somewhat mitigated by the quicker heating

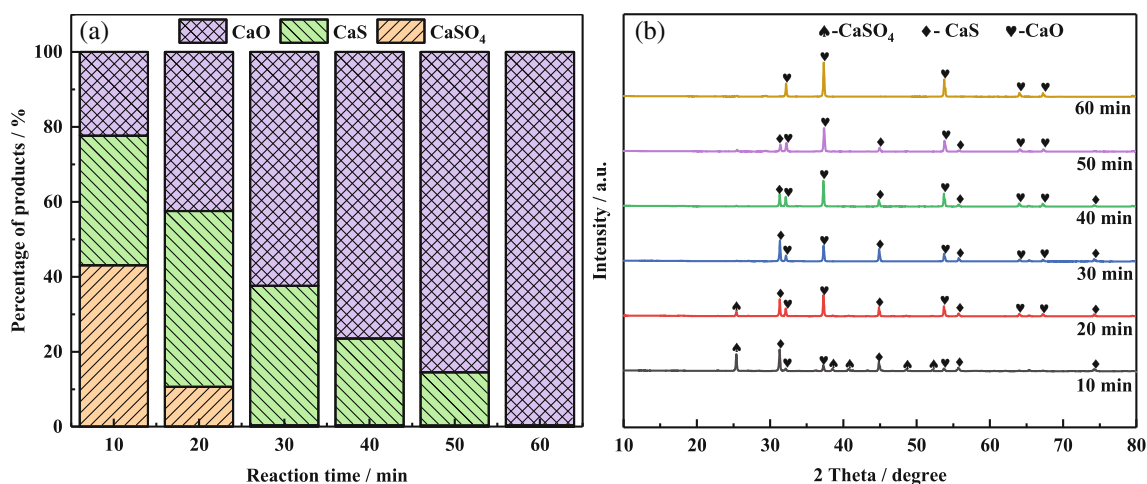


Figure 6. (a) Composition of CaSO_4 decomposition products at different reaction times, (b) CaSO_4 decomposition products' X-ray diffraction patterns at various reaction times.

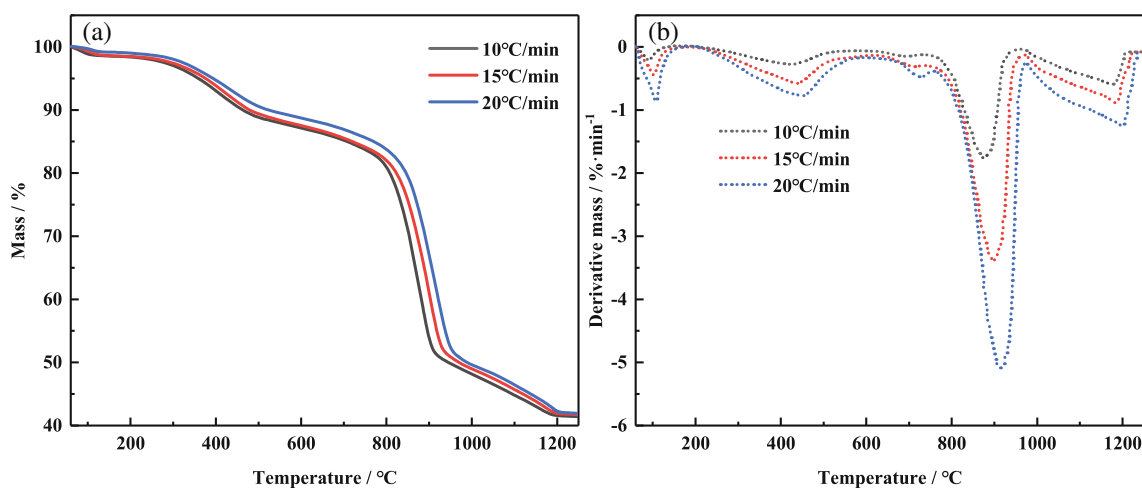


Figure 7. (a) Variation of mass with temperature at different heating rates, (b) Variation of derivative mass with temperature at different heating rates.

rate since it reduces the time needed for heat to pass between the sample's interior and exterior surfaces.²⁶ Figure 7(b) demonstrates five clear weight loss peaks that occur between 30 °C and 1250 °C. The first weight loss peak appears in the range of 30 ~ 200 °C, the second appears in the range of 300 ~ 400 °C, the third appears in the range of 700 ~ 800 °C, the fourth appears in the range of 800 ~ 950 °C, and the fifth appears in the range of 1100 ~ 1200 °C. The coal's moisture evaporating causes the first DTG peak. The thermal breakdown of coal, which results in the production of tar and reducing gases, is primarily responsible for the second DTG peak. The secondary reaction of coal to produce coke is the primary cause

of the third DTG peak.²⁷ The fourth DTG peak is related to the reaction between CaSO_4 and carbon with CO to produce CaS and CaO. The fifth DTG peak is attributed to the secondary reaction between CaS and CO_2 , generating CaO and SO_2 . The TG-DTG curves of $\text{CaSO}_4\text{--C--N}_2$ system are shown in Fig. 2(s). By comparing the always curves under both systems, it can be found that the first four weight loss processes are the same under both systems, and the difference is that the weight loss process after 1000 °C is missing under N_2 , so it can be clearly concluded that the weight loss after 1000 °C represents the process of releasing SO_2 by the reaction between CaS and CO_2 .

Table 3. Average activation energies and finger front factors of reactions in different temperature bands with Flynn-Wall-Ozawa (FWO) and Kissinger-Akahira-Sunose (KAS) methods

Temperature interval (°C)	FWO		KAS	
	Average E_a (kJ/mol)	Average $\ln A$ (s^{-1})	Average E_a (kJ/mol)	Average $\ln A$ (s^{-1})
800 ~ 900	394.54	39.81	393.19	39.72
950 ~ 1200	545.87	47.42	542.55	46.98

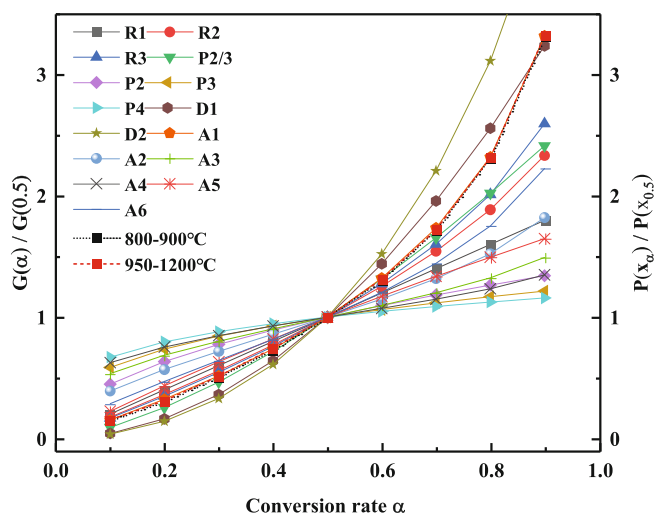


Figure 8. Comparison of theoretical and experimental curves of different reaction models.

Using the FWO and KAS techniques at 800 ~ 900 °C and 950 ~ 1200 °C, respectively, the activation energy (E_a) and pre-exponential factor ($\ln A$) for the reduction of CaSO_4 by coal to create CaO under CO_2 environment are estimated. The $\ln(\beta)$ vs. $1/T$ and $\ln(\beta/T^2)$ vs. $1/T$ curves derived using the FWO and KAS techniques at 800 ~ 900 °C and 950 ~ 1200 °C are shown in Fig. S3. As a result, Table 3's calculations of the typical E_a and $\ln A$ at 800 ~ 900 °C and 950 ~ 1200 °C are made. At 800 ~ 900 °C, the FWO and KAS techniques' average activation energies are respectively 394.54 kJ/mol and 393.19 kJ/mol. At temperatures between 950 and 1200 °C, the E_a for the FWO and KAS methods are 545.87 kJ/mol and 542.55 kJ/mol, respectively. In addition, E_a is positively correlated with $\ln A$ at different heating rates, which is caused by the dynamic compensation effect.²⁸

The relationship between E_a and conversion rate is seen in Fig. S4. At both temperature phases, it can be shown that the E_a reduces as the conversion rate rises. As a result, the reference point for the interval is chosen to be the conversion rate value of 0.5. The most likely mechanism function $g(\alpha)$ of the coal reduction process in a CO_2 atmosphere is identified using the integral master curve method, as shown in Fig. 8. As demonstrated in

Fig. 8, the theoretical master curve A1 and the actual master curves produced for both temperature stages in the range of 0.1 ~ 0.9 conversion rates are compatible. The relevant mechanism function is $g(\alpha) = -\ln(1 - \alpha)$, which is a part of the nucleation and growth model. From the model, at 800 ~ 900 °C, CaSO_4 comes into contact with coal and begins the reduction reaction. CaSO_4 is gradually transformed into CaS, leading to an increase in CaS nuclei.²⁹ When the temperature reaches 950 °C, the surface of CaS comes into contact with CO_2 and the reaction begins to generate CaO. As the reaction progresses, the CaO product layer gradually expands inward, and the unreacted CaS is encapsulated by CaO in the center. The process of CO_2 passing through CaO to react with the inner CaS involves overcoming a significant energy barrier, which raises the necessary activation energy.

Preparation of CaO from coal and CO_2 -reduced PG

Finally, industrial typical pollutants, PG and desilication PG are chosen as the research objects to investigate their reaction characteristics under the optimized conditions (1100 °C, C/Ca = 1.75, CO_2 concentration 7.5%). Previous studies have shown that cooling rate has a significant impact on the activity of CaO.³⁰ Therefore, this study compared the effects of rapid cooling of phosphogypsum (PRC), slow cooling of phosphogypsum (PSC), and desilication phosphogypsum with rapid cooling (DPRC) on the yield of CaO. The findings are displayed in Fig. 9. SiO_2 in PG interacts with CaO to create Ca_2SiO_4 , as seen in Fig. 9(a), which lowers the yield of CaO. The yield of CaO produced by PRC decomposition under these circumstances is 87.32%, but the yield of CaO produced by DPRC is 96.78%. In addition, under slow cooling, CaO continues to react with SiO_2 to form Ca_2SiO_4 , which further reduces the yield of CaO, as can be seen from the XRD pattern of the products in Fig. 9(b). Compared with slow cooling, the CaO peak under rapid cooling is significantly higher. Therefore, choosing rapid cooling is necessary to improve the yield of CaO. Table 4 displays the findings of the BET analysis used to describe the outputs of the two procedures in order to further confirm this. The specific surface area of CaO under PRC conditions rose from 1.24 m^2/g to 1.58 m^2/g , the pore volume grows from 0.0023 cm^3/g to 0.0064 cm^3/g , and the average pore size increases from 18.07 nm to 20.76 nm, as can be observed in comparison to PSC. This is due to the fact that under slow cooling

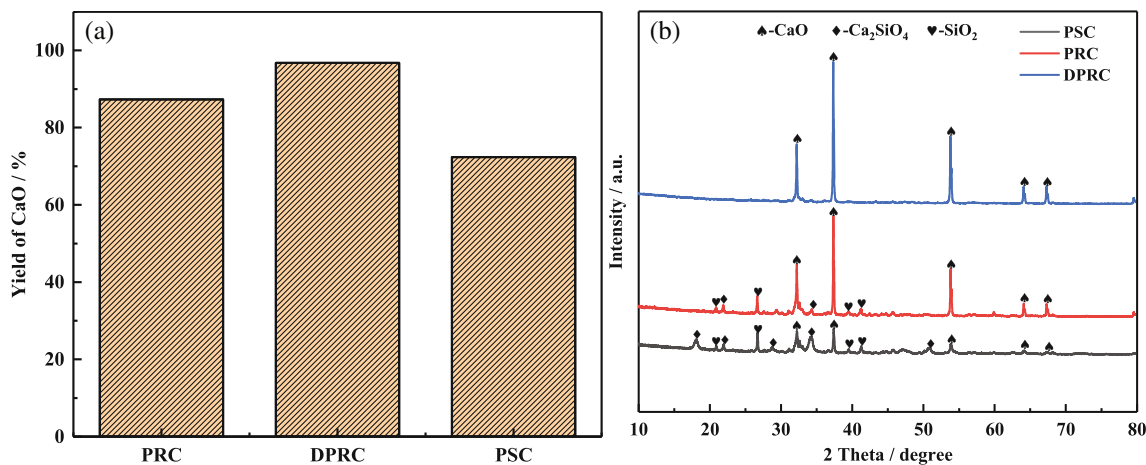


Figure 9. (a) CaO yields of phosphogypsum (PRC), desilication phosphogypsum (DPRC) and cooling of phosphogypsum (PSC) under optimized conditions, (b) X-ray diffraction patterns of the products.

Table 4. CaO yields and Brunauer–Emmett–Teller (BET) analysis results

Conditions	BET/ (m ² g ⁻¹)	Volume/ (cm ³ g ⁻¹)	Average pore size/nm
PSC	1.24	0.0023	18.07
PRC	1.58	0.0064	20.76
DPRC	1.72	0.0073	21.45

Abbreviations: DPRC, desilication phosphogypsum with rapid cooling; PRC, rapid cooling of phosphogypsum; PSC, slow cooling of phosphogypsum.

circumstances, CaO interacts with SiO₂, resulting in the collapse of the pore structure, and Ca₂SiO₄ aggregates on the reactant's surface, resulting in a reduction in pore size and specific surface area.³¹

CONCLUSION

In this study, lignite was used as a reducing agent under CO₂ atmosphere to explore the influences of reaction temperature, C/Ca molar ratio, and CO₂ concentration on the decomposition of CaSO₄ and preparation of CaO, using FactSage thermodynamic simulation and kinetic calculations to obtain the optimal reaction conditions. Finally, typical industrial gypsums, PG and desilicized PG, were used for experimental verification. The study found that adding CO₂ during the coal reduction of CaSO₄ significantly increased the CaO content in the product. Increasing the reaction temperature, C/Ca molar ratio, and CO₂ concentration all favored the decomposition of CaSO₄ into CaO. The ideal reaction conditions were 1100 °C, 1.75 C/Ca molar ratio, and 7.5% CO₂ concentration, which resulted in a maximum CaSO₄ decomposition rate of 99.63% and a maximum CaO yield of 99.28%. The generation of CaO occurred mainly through a two-step process, wherein coal reduction of CaSO₄ produced some CaS and CaO, and CaS continued to react with CaSO₄ to generate CaO. Moreover, CaS and CO₂ would react to produce CaO and SO₂ in the process. The nucleation and growth model was used for both phases, with a kinetic mechanism function of $g(\alpha) = -\ln(1 - \alpha)$. Finally, PG experiments verified the above conclusions, but SiO₂ in PG would react with CaO to produce a byproduct Ca₂SiO₄ and affect the CaO yield. The decomposition of PG produced 87.32% CaO under ideal experimental conditions, compared to 96.78% for desilicized PG. Slow cooling also reduced the CaO yield and the specific surface area of the product. This study will offer helpful advice for using CaSO₄ waste products like PG as resources.

ACKNOWLEDGEMENTS

Thanks for the financial support from the school-enterprise cooperation projects (No. 2019-KYY-508101-0078).

CONFLICTS OF INTEREST

There is no conflict of interest between the authors.

SUPPORTING INFORMATION

Supporting information may be found in the online version of this article.

REFERENCES

- Xiao YD, Jin HX, Wang ML and Guo YL, Collaborative utilization status of red mud and phosphogypsum: a review. *J Sustain Metall* **8**: 1422–1434 (2022).
- Wu FH, Ren YC, Qu GF, Liu S, Chen BJ, Liu XX *et al.*, Utilization path of bulk industrial solid waste: a review on the multi-directional resource utilization path of phosphogypsum. *J Environ Manage* **313**:114957 (2022).
- Wei ZQ and Deng ZB, Research hotspots and trends of comprehensive utilization of phosphogypsum: bibliometric analysis. *J Environ Radioact* **242**:106778 (2022).
- Bolan N, Sarmah AK, Bordoloi S, Bolan S, Padhye LP, Van Zwielen L *et al.*, Soil acidification and the liming potential of biochar. *Environ Pollut* **317**:120632 (2023).
- Chan CL and Zhang MZ, Effect of limestone on engineering properties of alkali-activated concrete: a review. *Construct Build Mater* **362**: 129709 (2023).
- Ma D and Wang QH, Experimental study of CaS preparation from lignite-reduced phosphogypsum in a fluidized bed. *J Chem Technol Biotechnol* **98**:756–772 (2023).
- Jia X, Wang Q, Cen K and Chen L, An experimental study of CaSO₄ decomposition during coal pyrolysis. *Fuel* **163**:157–165 (2016).
- Bi YX, Xu L, Yang M and Chen QL, Study on the effect of the activity of anthracite on the decomposition of phosphogypsum. *Ind Eng Chem Res* **61**:6311–6321 (2022).
- Suslikov AV, Zhirnov BS and Murtazin FR, A study of the kinetics of the reaction of petroleum coke with phosphogypsum to give calcium sulfide. *Chem Technol Fuels Oils* **57**:461–466 (2021).
- Liu Q, Ao XQ, Chen QL, Xie Y and Cao Y, Reaction characteristics and kinetics of phosphogypsum decomposition via synergistic reduction effect of composite reducing agent. *J Mater Cycles Waste Manage* **24**:595–605 (2022).
- Zhu K, Xie G, Chen Z and Wang Q, Reaction characteristics of phosphogypsum under carbon monoxide atmosphere. *J Chin Ceram Soc* **41**: 1540–1545 (2013).
- Yang XS, Zhang ZY, Wang XL, Yang L, Zhong BH and Liu JF, Thermodynamic study of phosphogypsum decomposition by sulfur. *J Chem Thermodyn* **57**:39–45 (2013).
- Song WM, Zhou JN, Wang B, Li S and Cheng RJ, Production of SO₂ gas: new and efficient utilization of flue gas desulfurization gypsum and pyrite resources. *Ind Eng Chem Res* **58**:20450–20460 (2019).
- Lian Y, Ma L, Liu H, Tang J, Zhu B, Ma G *et al.*, Experimental study on preparation of calcium sulfide via phosphogypsum and hydrogen sulfide reaction. *Chem Eng (China)* **44**:48–52 (2016).
- Xia X, Zhang L, Li Z, Yuan X, Ma C, Song Z *et al.*, Recovery of CaO from CaSO₄ via CO reduction decomposition under different atmospheres. *J Environ Manage* **301**:113855 (2022).
- Okumura S, Mihara N, Kamiya K, Ozawa S, Onyango MS, Kojima Y *et al.*, Recovery of CaO by reductive decomposition of spent gypsum in a CO-CO₂-N₂ atmosphere. *Ind Eng Chem Res* **42**:6046–6052 (2003).
- Xiao H, Zhou J, Cao X, Fan H, Cheng J and Cen K, Experiments and model of the decomposition of CaSO₄ under CO atmosphere. *J Fuel Chem Technol* **33**:150–154 (2005).
- Zhang XM, Song XF, Sun Z, Li P and Yu JG, Density functional theory study on the mechanism of calcium sulfate reductive decomposition by carbon monoxide. *Ind Eng Chem Res* **51**:6563–6570 (2012).
- Zheng SC, Ning P, Ma LP, Niu XK, Zhang W and Chen YH, Reductive decomposition of phosphogypsum with high-sulfur-concentration coal to SO₂ in an inert atmosphere. *Chem Eng Res Des* **89**:2736–2741 (2011).
- Xu P, Li H and Chen Y, Experimental study on optimization of phosphogypsum suspension decomposition conditions under double catalysis. *Materials* **14**:1120 (2021).
- Zhang Y, Yang Q, Liu Y and Guo Q, TG-FTIR study on phosphogypsum reduction with lignite under CO₂ atmosphere. *J Chem Eng Chin Univ* **30**:611–617 (2016).
- Antar K and Jemal M, A thermogravimetric study into the effects of additives and water vapor on the reduction of gypsum and Tunisian phosphogypsum with graphite or coke in a nitrogen atmosphere. *J Therm Anal Calorim* **132**:113–125 (2018).
- He HW, Hao LF, Fan CG, Li SG and Lin WG, A two-step approach to phosphogypsum decomposition: oxidation of CaS with CO₂. *Thermochim Acta* **708**:179122 (2022).
- Antar K and Jemal M, Recovery of calcium sulfide from Tunisian phosphogypsum and olive mill wastewaters: a thermogravimetric and kinetic study. *J Therm Anal Calorim* **147**:3931–3946 (2022).

- 25 Ma LP, Niu XK, Hou J, Zheng SC and Xu WJ, Reaction mechanism and influence factors analysis for calcium sulfide generation in the process of phosphogypsum decomposition. *Thermochim Acta* **526**: 163–168 (2011).
- 26 Chang Q, Pyrolysis characteristics and kinetic analysis of coal tar residue. *Acta Petrol Sin* **37**:924–931 (2021).
- 27 Zhu Y, Wang QH, Yan JQ, Cen JM, Fang MX and Ye C, Influence and action mechanism of pressure on pyrolysis process of a low rank Naomaohu coal at different temperatures. *J Anal Appl Pyrolysis* **167**:105682 (2022).
- 28 Sobek S and Werle S, Isoconversional determination of the apparent reaction models governing pyrolysis of wood, straw and sewage sludge, with an approach to rate modelling. *Renew Energy* **161**: 972–987 (2020).
- 29 Tian HJ and Guo QJ, Investigation into the behavior of reductive decomposition of calcium sulfate by carbon monoxide in chemical-looping combustion. *Ind Eng Chem Res* **48**:5624–5632 (2009).
- 30 Park TJ, Choi JS and Min DJ, Investigation of effects of SiO₂ content and cooling rate on crystallization in Fe₂O₃-CaO-SiO₂ system using in situ confocal laser scanning microscopy. *Metall Mater Trans B* **50**:790–798 (2019).
- 31 Yang J, Liu SY, Wang YF, Huang Y, Yuxin S, Dai QX *et al.*, Phosphogypsum resource utilization based on thermodynamic analysis. *Chem Eng Technol* **45**:776–790 (2022).